Effects of active gases on droplet transfer and weld morphology in pulsed-current NG-GMAW of mild steel

Guoqiang Liu [a, b], Xinhua Tang [a, b, *], Qi Xu [a, b], Fenggui Lu[a, b], Haichao Cui[a, b],

[a] Shanghai Key Laboratory of Materials Laser Processing and Modification, School of Materials Science and Engineering, Shanghai Jiao Tong University, Shanghai 200240, PR China

[b] Collaborative Innovation Center for Advanced Ship and Deep-Sea Exploration, Shanghai 200240, PR China

*Corresponding author at: Shanghai Key Laboratory of Materials Laser Processing and Modification, School of Materials Science and Engineering, Shanghai Jiao Tong University, Shanghai 200240, PR China.

E-mail address: xhtang@sjtu.edu.cn (X. Tang).

Abstract

Small amount of active gases CO_2 and O_2 were added into pure argon inert shielding gas to improve the weld formation of pulsed-current narrow-gap gas metal arc welding (NG-GMAW) of mild steel. Their effects on droplet transfer and arc behavior were investigated. A high-speed visual sensing system was utilized to observe the metal transfer process and arc morphology. When the proportion of CO_2, being added into the pure argon shielding gas, changes from 5% to 5%, the metal transfer mode changes from pulsed spray streaming transfer to pulsed projected spray transfer, while it remains the pulsed spray streaming transfer when 2% to 10% O_2 is added. Both CO_2 and O_2 are favorable to stabilizing arc and welding process. O_2 is even more effective than CO_2. However, O_2 is more likely to cause the inclusion defects in the weld, while CO_2 can improve the weld appearance in some sense. The weld surface

concavity, which is sensitive to the formation of lack-of-fusion defect in NG-GMAW, is greatly influenced by the addition of active gas, but the weld width and weld penetration almost keep constant.

Key Words

Metal transfer; Active gases; Pulsed-current NG-GMAW; Weld morphology;

1.Introduction

Thick and large structural components are widely applied in various fields, such as offshore drilling platforms, shipbuilding, high-pressure vessels, and nuclear industry. Narrow-gap gas metal arc welding (NG-GMAW) is a preferential technology in manufacturing such components owing to its great advantages such as less filler metal, higher productivity, low heat input and minimal welding distortion. However, the lack-of- sidewall-fusion is the most common defect in NG-GMAW joints. It greatly weakens the mechanical properties of weld joints. The convex surface of weld bead in narrow-gap groove is also harmful to the multi-pass weld formation and has been proved the main reason to the occurrence of lack-of-fusion defect and inclusion defect. To improve the weld formation of NG-GMAW, plentiful progressive approaches, such as adopting a swing arc or a rotating arc, using external magnetic field, have been put forward.

Cui et al. adopted a swing arc method to the narrow-gap welding in horizontal position and achieved a sound weld joint [1]. He pointed that increasing swing frequency and swing amplitude of arc were beneficial to increasing weld bead width

and sidewall penetration in narrow groove. Guo et al. employed a rotating arc method to NG-GMAW in horizontal position and studied the defect formation mechanism [2]. His work indicated that the rotating arc could effectively reduce undercut defect and convex surface defect. Wang et al. developed an alternating magnetic field to assist the arc welding in narrow groove, and successfully obtained a larger sidewall penetration with a magnetic flux density up to 6 mT [3]. However, all of these methods mentioned above need additional devices to realize expected arc movement in welding process, which means more investment. It is of great significance to exploit a cost-effective method to improve the weld formation of NG-GMAW. As is known, shielding gas is an essential influence factor to GMAW process. A proper shielding gas can be beneficial to keeping stable arc combustion and metal transfer process, and to reducing welding defects. NG-GMAW is actually an improved technology based on the conventional GMAW. Its process is also greatly affected by shielding gas. Argon is the most commonly used shielding gas in arc welding, since it has no reaction with the molten metal, and has low ionization potential that is good for the arc stability. However, in arc welding of ferrous metal, the pure argon may cause the molten pool metal low humidity thus to result in lack-of-fusion defects in welding joint. To achieve better joint performances, varieties of mixtures with inert and active gases were developed. Sathiya et al. studied the influence of shielding gases on the weld shape of a hybrid welding [4]. They found that when 5% O_2 was added into the mixture shielding gas of 50% He + 45% Ar, or when 10% N_2 was added into the mixture shielding gas of 45% He + 45% Ar, the weld bead became deeper and narrower, because oxygen and nitrogen could

suppress the plasma plume in welding process. Huang reported that adding nitrogen into an argon-based shielding gas would increase the heat input [5]. Both the weld penetration and weld area increased with increase of nitrogen in argon-based shielding gas. Meanwhile, the angular distortion decreased. Zong et al. studied the influence of shielding gas on undercut defects in GMAW and found that the undercut defects could be significantly reduced by increasing the CO_2 content [6]. However, when the CO_2 content was higher than 20%, welding spatters occurred frequently on the weld bead surface.

Jonsson et al. developed a computational model to investigate the effects of oxygen on GMAW process [7]. He found that the added oxygen affected the thermo-physical properties of shielding gas mixtures and the surface tension, which finally determined the arc characteristics and the flow pattern of welding pool. Wang et al. applied an in-house simulation model to evaluate the GMAW process shielded by gas mixtures of argon and CO_2 [8]. The results indicated that the added CO_2 brought about a strong constriction effect on arc. Tušek et al. studied the effect of hydrogen content added in argon on GMAW of stainless steel [9]. They reported that the more hydrogen was added into argon, the higher arc resistance and arc energy would be. The volume of melted base metal increased greatly with increase of hydrogen in argon. These resulted from the higher ionization energy and the higher thermal conductivity of hydrogen comparing to argon. Cai et al. evaluated the effect of ternary mixtures of Ar +He +CO_2 on metal transfer in narrow-gap tandem GMAW, and showed that when CO_2 was kept at 10%, the metal transfer always remained a pulsed spray transfer, no matter how the

helium content varied in a certain range [10]. Pires et al. studied the metal transfer mode in GMAW shielded by gas mixtures with varied argon, CO_2 and O_2 contents [11]. They found that increasing active gas in mixtures resulted in a shrinkage of parameter range for spray transfer. For ternary gas mixtures of Ar+CO_2 +O_2, both short-circuit transfer and spray transfer occurred in a wide range of welding current and voltage. Wong at al. adopted Taguchi method to evaluate the effects of shielding gas on dynamic metal transfer in GMAW [12]. They reported that the spray transfer mode could occur by changing the current and voltage in welding with Ar+5%CO_2, while only short-circuit transfer or globular transfer was obtained in welding with pure CO_2 gas, no matter how the welding parameters were changed.

It can be concluded that shielding gases are of vital importance to weld morphology, droplet transfer and defect reduction throughout the GMAW process. NG-GMAW is an improved technology, which has great potential in welding thick and large structural components. The most efforts of previous researches on NG-GMAW were made to improve sidewall fusion by using extra expensive mechanical devices. However, a proper selection of shielding gases can be an economical effective way to solve this problem, which is favorable to realizing stable droplet transfer and attaining sound weld joints. In this research, a series of welding experiments were carried out to evaluate the effects of varied gas compositions on the metal transfer and weld morphology in pulsed current NG-GMAW of ferrous metal, to find the most proper mixed shielding gas for welding under narrow groove condition.

2.Experimental procedure

Fig. 1(a) briefly shows the schematic diagram of welding experiment system setup, in which a new-designed narrow-gap GMAW torch was applied. A high-speed video camera was used to observe arc profile and droplet transfer process. Its frame rate was 3000 fps and the exposure time was 1.0 μs. An optical filter was used to block the arc light while capturing the droplet transfer process. The waveforms of welding current and arc voltage were detected by hall sensors and were sampled by a data acquisition system (DAS). Its sampling rate was 20 kHz. The welding experiments were conducted on the specimens of commercial quality hot-rolled steel Q345d, and ER50-6 wire with a diameter of 1.2 mm was used as filler metal. Their chemical compositions are given in Table 1. The specimens were machined into dimension of 100 mm (length) × 40 mm (width) × 35 mm (height) with a groove as shown in Fig. 1(b). A power source working in direct-current electrode positive (DCEP) was applied to welding process, which was set in single pulse mode, as shown in Fig. 1(c). Different kinds of shielding gases were adopted, which are mainly the mixtures of argon and CO_2 or O_2 respectively. The CO_2 content varied from 5% to 5% in the gas mixtures of Ar + CO_2, while the O_2 content changed from 2% to 10% in the gas mixtures of Ar +O_2. The gas flow-rates through the external shielding gas hood and the nozzle of welding torch were both 30 L/min. The welding current was 350 A, the arc voltage was 34 V, and the travelling speed was 300 mm/min. The wire extension was about 15 mm.

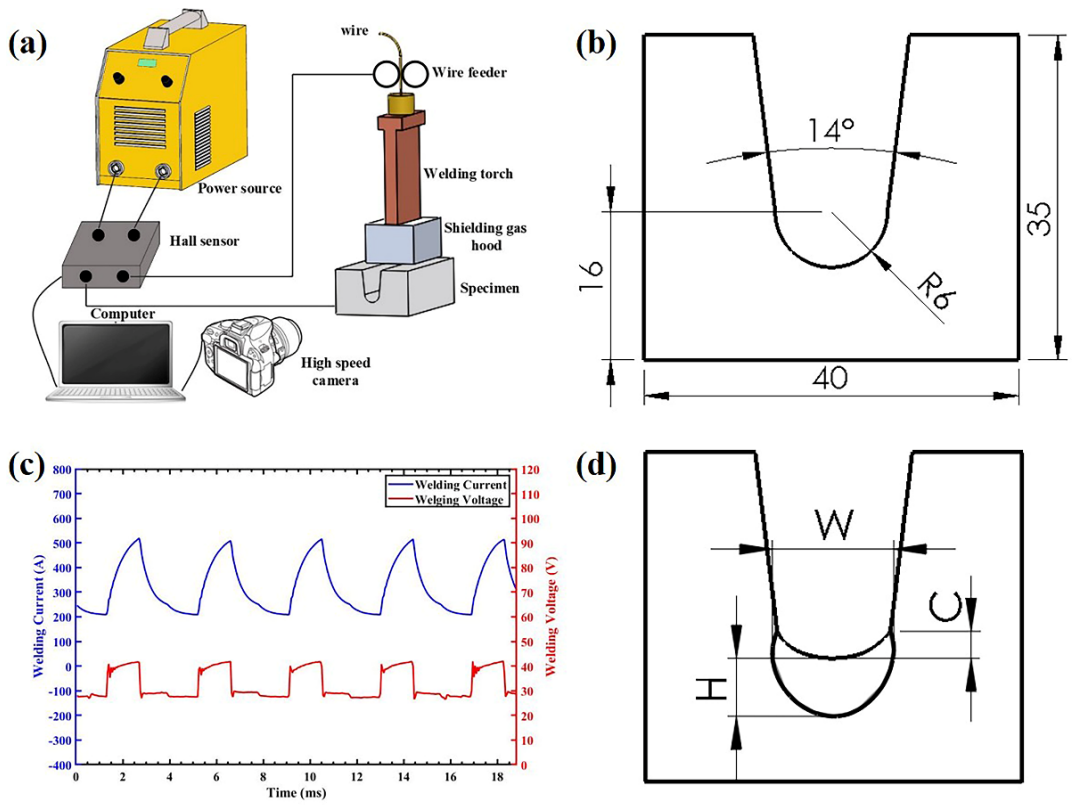

Fig. 1 (a) The schematic diagram of welding experiment system setup; (b) cross section dimension of specimen and its narrow-gap groove; (c) welding current and arc voltage waveforms; (d) characterization for first-pass weld bead of NG-GMAW.

Table 1 Nominal chemical compositions of base metal and filler metal (wt %)

Material	Elements (wt %)												
	Mn	Si	Ni	Cr	Ti	Al	V	S	P	Mo	Cu	C	Fe
Q345D	1.45	0.27	0.07	0.05	0.05	0.02	0.01	0.01	—	—	—	≤0.18	Bal.
ER50-6	1.40-1.85	0.80-1.15	≤ 0.15	≤ 0.15	—	—	≤ 0.15	≤ 0.025	≤ 0.025	≤ 0.15	≤ 0.5	0.06-0.15	Bal.

For investigation of welding process in a deep and narrow groove with varied gas mixtures, only the first pass of weld bead was deposited on each specimen. After welding, all the specimens were cut along the transverse direction of welding bead. Each specimen was polished and then was etched with 4% Nital solutions (4% nitric acid in alcohol). The weld bead was characterized by weld width (W), weld penetration (H) and weld surface concavity (C) for evaluating the influence of varied gas mixtures

on the weld morphology, as shown in Fig. 1(d). In addition, the arc shape was also characterized by arc width and arc length.

3. Results and discussion

3.1 Effects of shielding gas on arc shape and metal transfer

Fig. 2 presents the variation of arc profile under shielding of gas mixtures with varied CO_2 content. It indicates that the arc shape experiences large changes with increased CO_2 content. When the CO_2 content in the shielding gas is 5%, the arc extends even to the sidewalls of groove, which signifies that more heat is transmitted to the sidewalls and the welding pool is enlarged. The arc experiences a fluctuation in the range of welding current from base to peak. The fluctuation of arc is consistent with the current variation. The arc is cone-shaped at the base current, and bell-shaped with the arc edge upward warped at the peak current. The upward warp of arc mainly results from the restrain effect of narrow gap groove. The arc profiles under shielding gas of Ar+5% CO_2 and Ar+10% CO_2 are correspondingly similar at both base and peak current. However, when the CO_2 content in the shielding gas is 25%, the arc keeps the same conical shape through the whole pulse cycle, except for the change of its size.

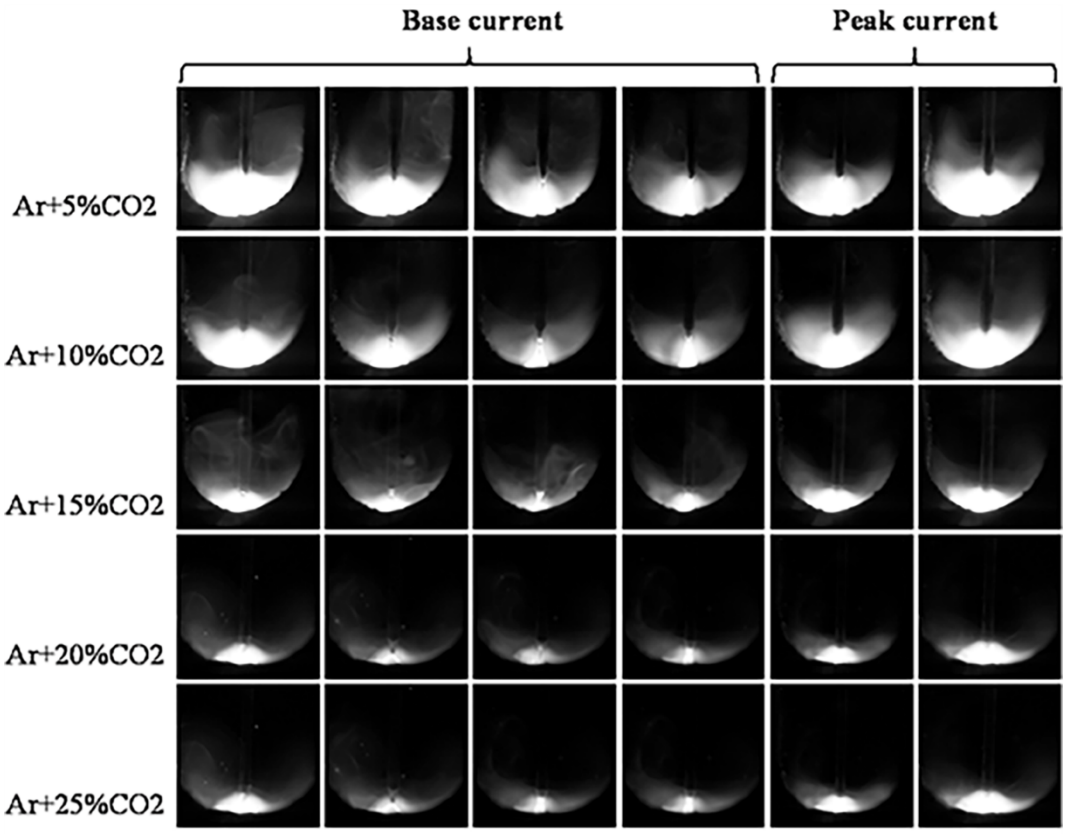

Fig. 2 Variations of arc profile under shielding of gas mixtures with varied CO_2 contents

The effect of O_2 on the arc profile is shown in Fig. 3. When the O_2 content in the shielding gas is 2%, the arc profile changes greatly comparing to that of any other gas mixtures mentioned above. The arc looks much like conical shape at the peak current, but slender bell-like shape at the base current. When O_2 is added up to 5% and 10%, the arc turns to be conical shape at the base current, and bell shape at the peak current, which is similar to that of gas mixtures with 5% or 10% CO_2 contents. As shown in Fig. 2 and Fig. 3, in comparison with conventional GMAW, the sidewalls of narrow gap groove have strong restraint on the welding arc. Due to the special designed groove, the arc could not extend freely, and has no choice but to climb up when touching the sidewalls. The narrow gap groove leads to more concentrated arc energy.

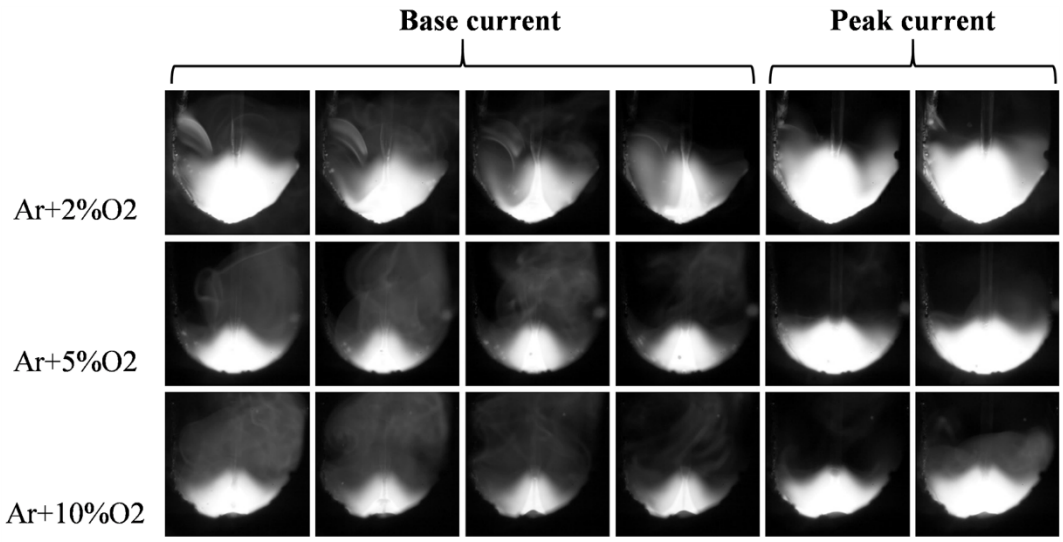

Fig. 3Variations of arc profile under shielding of gas mixtures with varied O_2 contents

The detailed arc profile characteristics such as arc length, arc width and arc area at the peak current for varied contents of CO_2 and O_2 in shielding gas are displayed in Fig. 4(a) and (b) separately. An overall tendency is that all of them fall off with the increase of CO_2 or O_2. On the one hand, both CO_2 and O_2 are active gases, which is beneficial to stabilizing the cathode spot and obtaining a stable arc combustion when proper contents of them are added into the pure argon. On the other hand, the temperature of arc edge is approximately 10000k, where the thermal conductivity of oxygen is 1.21 W/ m·K while the thermal conductivity of pure argon is only 0.66 W/ m·K presented by Murphy et al. [13]. Wang et al. reported that the thermal conductivity of CO_2 is 1.47 W/m·K at the same temperature [8]. Therefore, when proper small amount of CO_2 or O_2 is added into the pure argon, the thermal conductivity of arc gets higher, which results in more uniform heat distribution and expansion of arc. However, much higher content of CO_2 also means more heat loss by conduction of arc because of its higher thermal conductivity. Meanwhile, CO_2 and O_2 are polyatomic molecules and need to be dissociated firstly before ionizing, as shown in Table 2, which means more

energy needs to be consumed to ignite the arc. In addition, the decomposition and ionization of CO_2 will generate more ions to increase the arc electric field intensity, which results in increased electromagnetic force. When the CO_2 or O_2 content in the shielding gas gets higher, the thermal pinch effect together with increased electromagnetic force constricts the arc, and the arc gets difficult to expand.

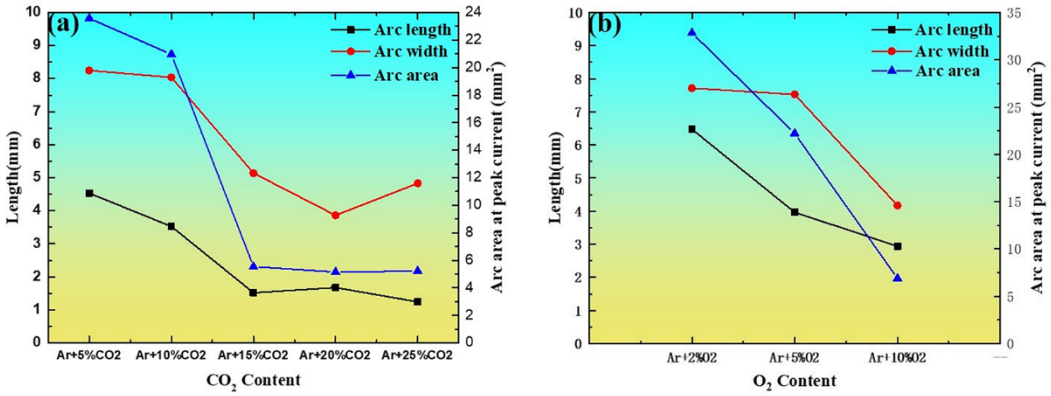

Fig. 4Variations of arc length, arc width and arc area under shielding of gas mixtures with (a) varied CO_2 contents, and (b) varied O_2 contents

In light of above analysis, the shielding gas composition has a great impact on arc shape and its stability. Actually, it also plays a key role in metal transfer process of welding. When the shielding gas is changed to Ar+5% CO_2 or Ar+10% CO_2, the metal transfer has similar features at same pulsed-current. Fig.5 presents the pulse streaming spray transfer in welding with both shielding gas mixtures. The wire tip turns to be a tapered shape that represents a typical feature for streaming spray transfer. It is encircled by the arc, and is adequately heated to become plastic. As a result, a slender long molten neck hanging on the wire tip is formed and directs towards the weld pool. At the wire tip, a droplet with the diameter closing to the wire diameter is transferred from a cone-shaped wire tip into the welding pool in spray way. In addition, the arc jumping phenomenon along with the long neck is also observed in Fig.5, and the current

at this moment is defined as the transition current of streaming spray transfer.

Table 2 Chemical and physical properties of gases used in pulsed current NG-GMAW

Shielding gas	Density at 15 ℃ 1 bar(kg/m^3)	Dissociation energy eV/molecule	First ionization energy eV/molecule	Chemical activity
Ar	1.669	0	15.8	Inert
CO_2	1.849	4.3	14.4	Oxidizing
O_2	1.337	5.1	13.6	Oxidizing

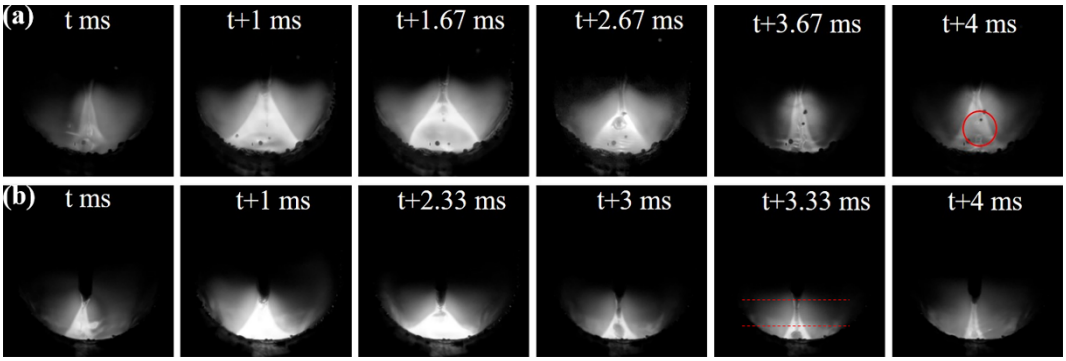

Fig.5 Metal transfer process under shielding of gas mixtures of (a) Ar+5% CO_2 (b) Ar+10% CO_2

In pulsed streaming transfer process, it can be seen that a plenty of small spatters are produced in the shielding gas mixture of Ar+5% CO_2 as shown in Fig. 5(a). This is owing to the relatively long arc in Ar+5%CO_2, which means lower arc stiffness. It brings about arc fluctuation, and thus the force balance of the radial component of the electromagnetic force is easy to be broken. One more to note is the arc jumping phenomenon which took place at t+2.67 ms and t+4 ms as shown in Fig. 5(a). The arc root is firstly located at the bottom of neck as shown in Fig. 6(a), and gradually climbs to the top of the neck which becomes longer and thinner as shown in Fig. 6(b). At the same time, the arc also changes to conical shape. The longer and thinner neck is surrounded and directly heated by the arc, and thus leads to a large anode-spot pressure acting on the thinner neck. Under the combined action of the anode-spot pressure and unbalanced electromagnetic force, the neck gets unstable. Under this condition, when

the droplet is transferred to welding pool, the neck is broken at one point on the neck rather than on the wire tip. This causes the generation of small droplets, which ultimately forms spatters rather than is transferred into the welding pool (as shown in Fig. 6(c)).

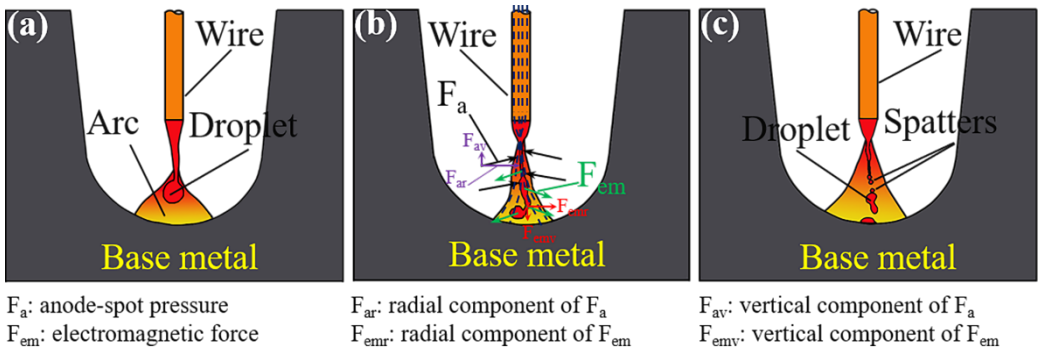

Fig.6 Schematic illustration of arc jumping phenomenon: (a) arc surrounding the bottom of droplet (b) force analysis when arc climbs to the top of neck. (c) droplet transfer after arc jumping.

With CO_2 increasing to 15%, it can be observed in Fig. 7(a) that the neck is shorter than that in the shielding gas mixture of Ar+5% CO_2 or Ar+10% CO_2 as shown in Fig. 5, the metal is transferred in projected spray-like transfer mode. When Ar+20%CO_2 or Ar+25%CO_2 is applied, the metal is transferred in projected spray transfer mode as shown in Fig. 7(b) and (c), in which a droplet diameter is roughly equal to the wire tip diameter. When the CO_2 content is relatively low (5% or 10%), the energy for arc ignition is just a little higher than that in the pure argon, and so is the heat loss because of its high thermal conductivity. However, when CO_2 content increases up to 25%, the thermal conductivity gets great improvement, consequently, the heat loss increases sharply, and so does the energy for arc ignition. Moreover, the variation of arc behavior mentioned above also have a great impact. The arc just hangs on the droplet without climbing up to the wire. Consequently, the energy for heating the wire tip is not enough

to form a streaming.

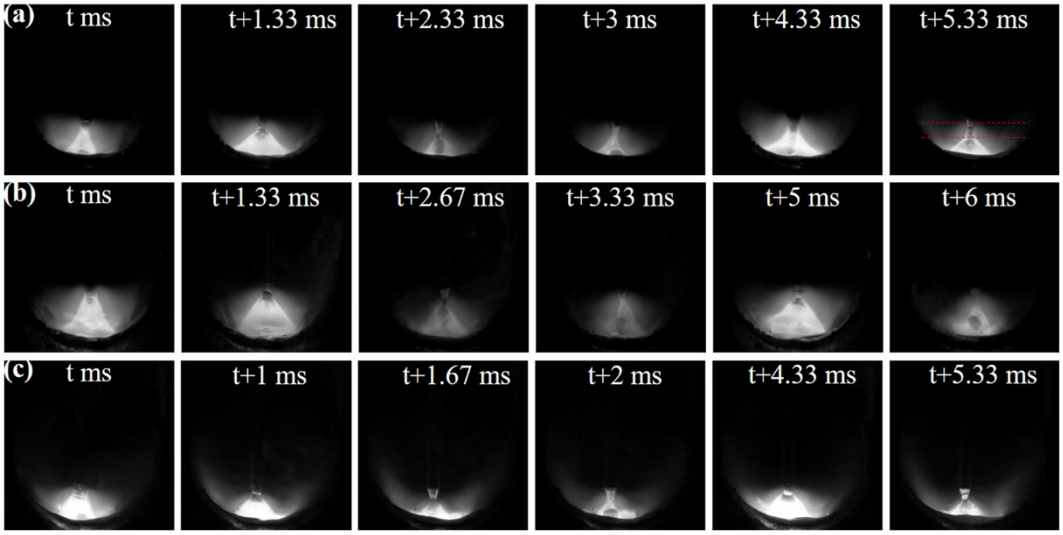

Fig. 7 Metal transfer process under shielding of gas mixtures of (a) Ar+15% CO_2; (b) Ar+20% CO_2; (c) Ar+25% CO_2

The droplet transfer mode is apparently influenced by different arc behaviors under varied shielding gases, and it is virtually influenced by the force distribution on the droplet. The force balance theory claims that a droplet will detach from the electrode tip when the detaching forces exceed the retention forces. Generally, four different forces are considered in the metal transfer of arc welding. The surface tension is a retention force, while the gravity, the plasma drag force and the electromagnetic force are detaching forces. Nemchinsky [14] prosposed that the drag force is not important during droplet transfer process at high currents. According to Scotti et al. [15], the electromagnetic force is the governing force during both projected spray and streaming spray transfer, and its induced pinch effect limits the droplet. So more attention is put on surface tension and electromagnetic force.

The gravity F_g in flat position welding is given by Kim and Eagar as below [16]:

$$F_g = {}^4/_3 \pi {r_d}^2 \rho_d g \quad (1)$$

where r_d is the droplet radius, ρ_d is the mass density of the droplet, and g is the gravitational acceleration. The surface tension can be expressed as follows:

$$F_\gamma = 2\pi R_e \gamma \tag{2}$$

where R_e is the radius of the electrode and γ is the surface tension coefficient of the liquid metal, which is significantly influenced by the O_2 content in a binary Fe-O system according to Sahoo et al. [17].

The plasma drag force on the droplet is given by [18]:

$$F_d = C_d \frac{1}{2} \rho_g {v_g}^2 \pi {r_d}^2 \tag{3}$$

Where C_d is the drag coefficient, ρ_g is the plasma gas density, v_g is the gas velocity and r_d is the radius of the droplet.

The vertical component of electromagnetic force suitable for the droplet transfer is given by Amson as follows [19]:

$$F_{emv} = \frac{\mu_0 I^2}{4\pi} \left(\frac{r_d}{r_w}\right)^2 f \tag{4}$$

$$f = \frac{1}{4} - \left(\frac{3}{2} - \ln 4\right)\left(1 + \frac{l_d}{r_d}\right)^{-2} \tag{5}$$

where μ_0 is the permeability in free space, I is the welding current, r_d is the radius of the droplet, r_w is the radius of the wire and l_d is the length of the radius.

Fig. 8 illustrates the arc behavior and force distribution for streaming spray transfer and projected spray transfer, separately. The arc area in streaming spray transfer mode with low CO_2 content (5% or 10%) is larger than that in projected spray transfer mode with high CO_2 content (20% or 25%), which provides the wire tip with more heat. The wire tip is sharper in streaming spray than in projected spray. Considering the similar

gas property, the surface tension of the liquid metal is similar and the difference of F_γ is not distinguishable. According to equation (4) and (5), F_{emv} in Fig. 8(b) is larger than that in Fig. 8(a). However, due to the sharper wire tip, the radial component of the electromagnetic force F_{emr} acting on the droplet in Fig. 8(a) is huge, to cause a droplet to subject a strong pinch effect, so the droplet is not able to grow to a massive volume.

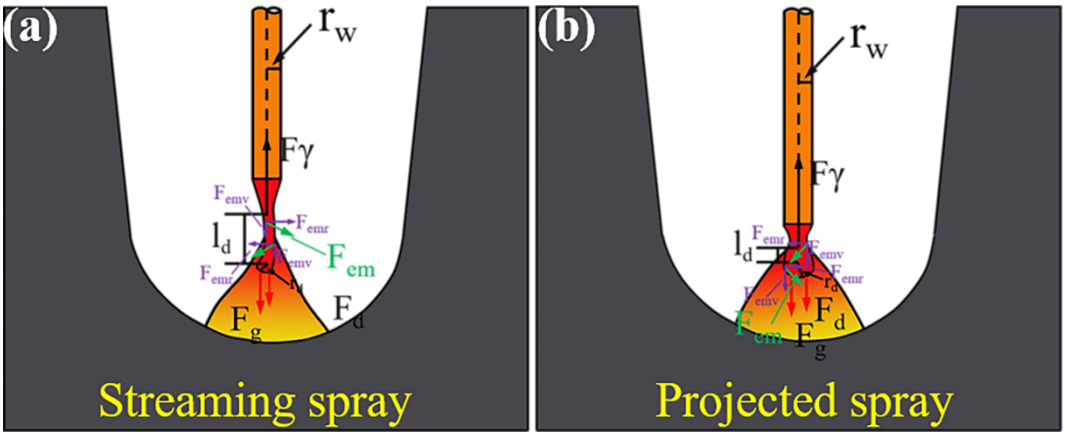

Fig. 8 Schematic illustration of arc behavior and forces for (a) streaming spray transfer mode with low CO_2 content and (b) projected spray transfer mode with high CO_2 content

When varied O_2 contents are added into pure argon, the metal transfer takes on a similar variation trend to that of CO_2 being added into pure argon, as shown in Fig. 9. For all shielding gas mixtures, the metal is transferred in pulse streaming spray transfer mode. When O_2 increases from 2% to 5%, a long neck and a taper-shaped wire tip are found in both cases. The long neck is broken at the junction of the neck and the wire tip, and subsequently a big droplet accompanied by some small droplets transfers into the welding pool. And the arc jumping phenomenon accompanies the streaming spray transfer mode. Spatters are seen in Fig. 9(b) and (c). The explosive droplet transfer is observed in Fig. 10(c) (at t+2.67 ms). This may be ascribed to the received heat in

droplet and the pinch effect of large radial electro-magnetic force. The O_2 content increases the energy for arc ignition and the heat loss because of its high thermal conductivity, which brings about a greater constriction for the arc. Therefore, the current density becomes higher in arc root, and so does the temperature in arc center. On the other hand, O_2 is a kind of active gas that is easy to react with the metal elements in wire. Lots of heat is released by the exothermic reactions. The droplet can be heated to a higher temperature to cause an explosive droplet transfer.

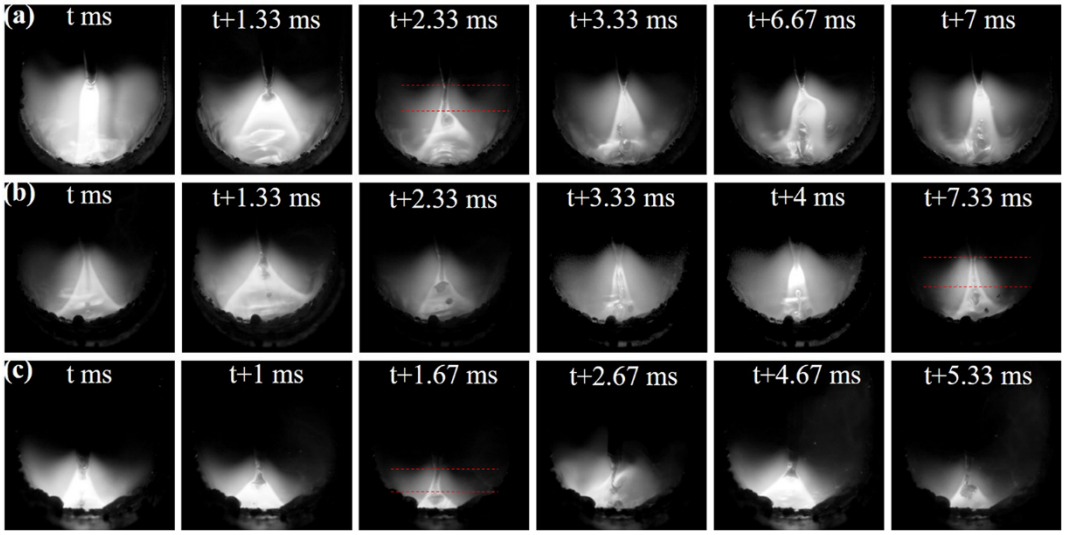

Fig. 9 Metal transfer process under shielding of gas mixtures of (a) Ar+2% O_2; (b) Ar+5% O_2; (c) Ar+10% O_2

3.2 Effects of shielding gas on welding current and voltage

Fig. 10 shows the welding current and voltage waveforms for varied contents of CO_2 in the shielding gas. When the CO_2 content is 5%, the welding current and arc voltage waveforms are not stable at the initial stage of the welding process. Some extremely-high peaks appear at this stage as shown in Fig. 10(a). As the CO_2 content increases to 10% or more, only few high peaks appear, which illustrates that the welding process becomes more stable. The high peaks in welding current waveforms represent

the occurrence of short-circuit. The valley values (less than 10 V) in arc voltage waveforms are caused by the decreased arc length when the droplet is transferred to the welding pool. As shown in Fig. 10, with increasing CO_2 content, the valley values obviously increase, even when the welding process is are very stable.

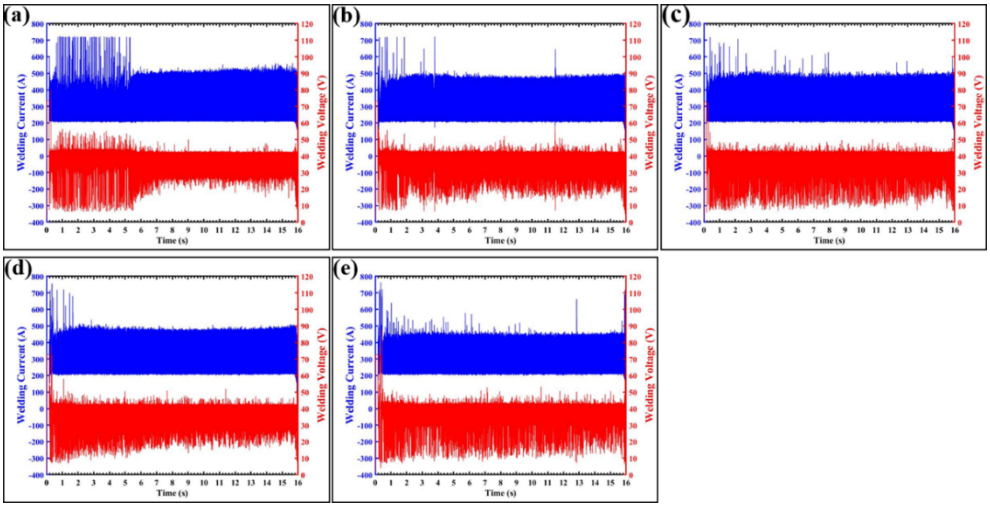

Fig. 10 Current and voltage waveforms under shielding of (a) Ar+5% CO_2; (b) Ar+10% CO_2; (c) Ar+15% CO_2; (d) Ar+20% CO_2; (e) Ar+25% CO_2

Fig. 11 displays the welding current and voltage waveforms for varied O_2 contents in the shielding gas. It plays a same role in stabilizing the welding process. The effect of O_2 is even more obvious due to its stronger oxidizing property. When about 2% O_2 content is added into the shielding gas, the welding process is similar to that shown in Fig. 10(a). With O_2 content further increasing to 5% and 10%, the high peaks no longer appear as shown in Fig. 11(b) and (c). It is worthwhile to note that the voltage signal is more effectively stabilized by the same content of O_2 than CO_2.

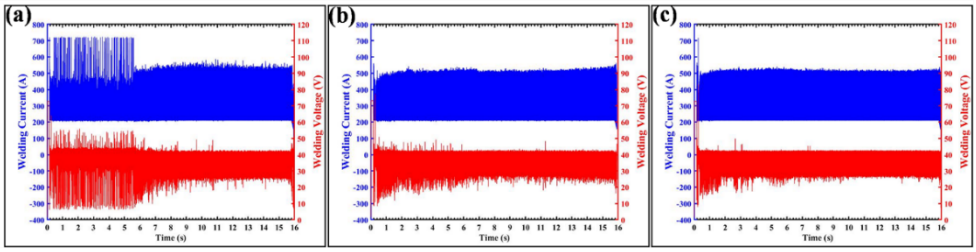

Fig. 11Current and voltage waveforms under shielding of (a) Ar+2% O_2; (b) Ar+5% O_2; (c) Ar+10% O_2

Fig. 12(a) displays the root-mean-square (RMS) current and voltage of welding in shielding gas with varied CO_2 contents. When the CO_2 content is in the range from 5% to 25%, the RMS current shows a slight fluctuation first and then decreases while the RMS voltage first declines mildly and then takes on an obvious rising trend. When the CO_2 content varies from 5% to 15%, the dissociation of CO_2 needs more energy, and meanwhile, the thermal conductivity of shielding gas also increases, which means more conductive energy loss. The increased total energy loss leads to constricting arc profile to make an energy balance. Therefore, the electron density of arc plasma has no significant changes, and so does the RMS current. The variation of arc length improves its potential gradient to maintain the arc stability. Therefore, the RMS voltage changes a little. With the CO_2 content further increasing to 25%, the energy loss continues to increase, and thus the ionization degree of shielding gas decreases, which results in the decrease of RMS current. To maintain a stable arc combustion, the RMS voltage increases eventually. Fig. 12(b) shows the RMS current and voltage of welding in shielding gas with varied O_2 contents. The RMS current slightly increases while the RMS voltage decreases with the increase of the O_2 contents. O_2 has stronger oxidizability. Lots of heat is released by the exothermic reactions between O_2 and the metal elements of wire, as mentioned above. When the O_2 content is low, the ionization degree of shielding gas increases with increasing O_2 content, leading to increasing RMS current. In addition, the RMS current in shielding gas with certain O_2 content is larger than that in shielding gas with same CO_2 content. It is proved that the decrease of CO_2 could lower the transition current of projected spray transfer or streaming spray transfer.

In other words, it is easier to obtain streaming spray transfer or projected spray transfer in the shielding gas with low CO_2 content.

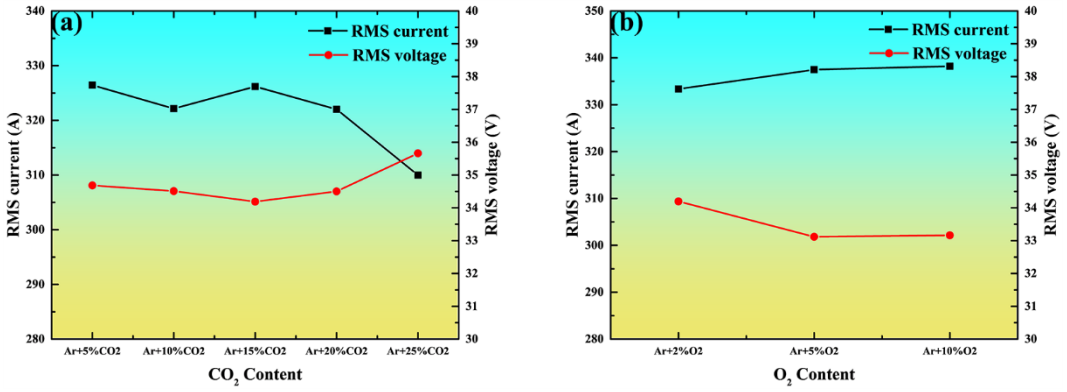

Fig. 12 Variations of RMS current and voltage under shielding of gas with (a) varied CO_2 contents and (b) varied O_2 contents

3.3 Effects of shielding gas on weld morphology

Fig. 13 shows the first weld bead appearances and their cross-sections of NG-GMAW under different shielding gases. When the CO_2 content is 5%, the weld bead surface is fluctuant, which may result from the random fluctuation of welding pool due to the unstable pulse streaming spray mode at the initial stage. When the CO_2 content increases to more than 5%, the weld bead appearance becomes smooth. When the O_2 content in the shielding gas gets up to 2%, the weld bead appearance is similar to that for the shielding gas of Ar+5% CO_2. In this case, the arc is long and its arc stiffness is relatively low. Hence, a droplet may not directly fall into the welding pool along the axis direction, as it is prone to be influenced by the anode spot force and other forces. When the O_2 content is 5%, some slags appear on the surface of the weld, distributing mainly along the centerline. With the O_2 content increasing to 10%, there are more slags on the weld surface. It is very difficult to remove the slags in NG-GMAW. Even a few

slags on the weld bead surface may cause inclusion defects or lack-of-fusion defects in subsequent multi-pass welding process, which will seriously damage the mechanical properties of the welding joint. Therefore, the shielding gas mixture with O_2 content over 5% is not suggested, although it can greatly improve the arc stability and the welding process.

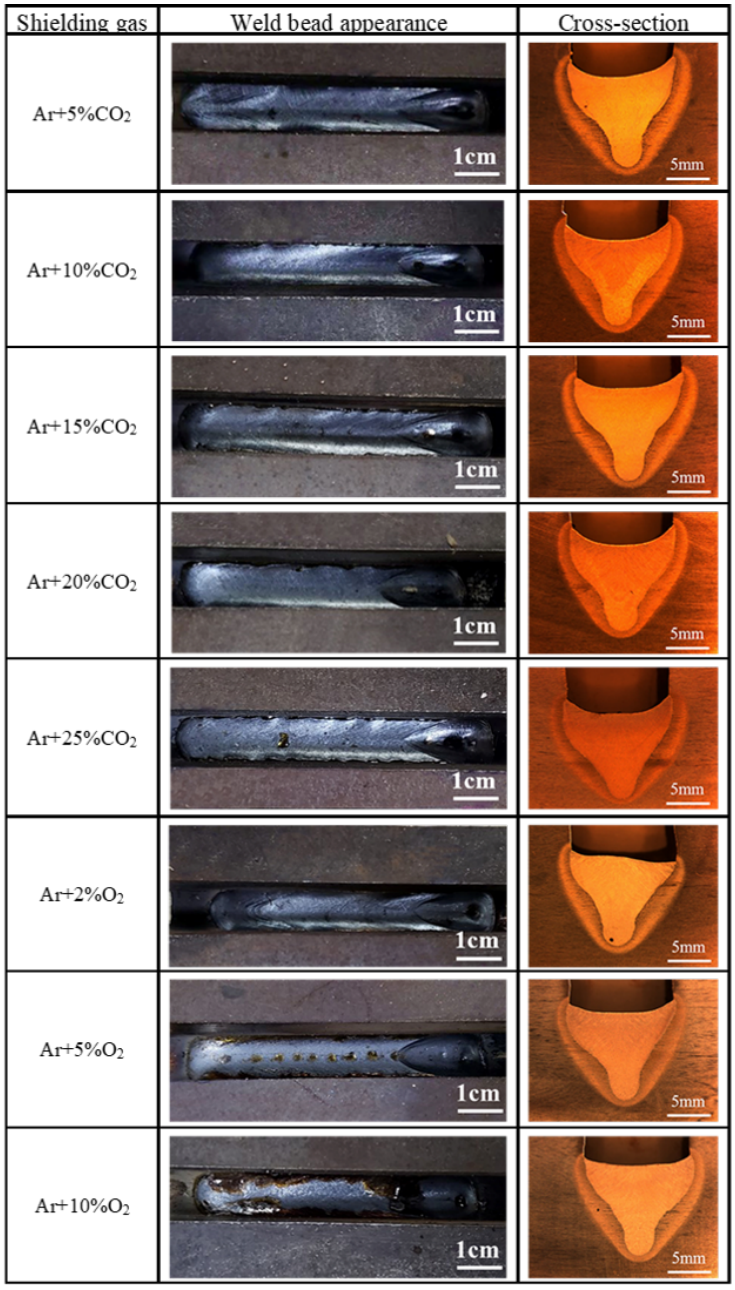

Fig. 13Macrographs of weld appearance and cross-section under different shielding gases

The finger penetrations are obtained for all the shielding gas mixtures. The weld

bead surface in Ar+2% O_2 shielding gas mixture is nearly flat and an undercut defect occurs, while the weld bead surfaces in other shielding gas mixtures appear to be concave. There is no lack-of- sidewall-fusion defect, and enough sidewall penetration is obtained for all weld beads. The weld width, the weld penetration and the weld surface concavity obtained in the shielding gases with varied CO_2 and O_2 contents are presented in Fig. 14. Both the weld width and the weld penetration for all shielding gas mixtures are similar. The weld surface concavity can be evaluated based on the cross-section of the weld beads. It is in the range from 1.0 to 2.0 mm, which means a concave-shape weld bead surface.

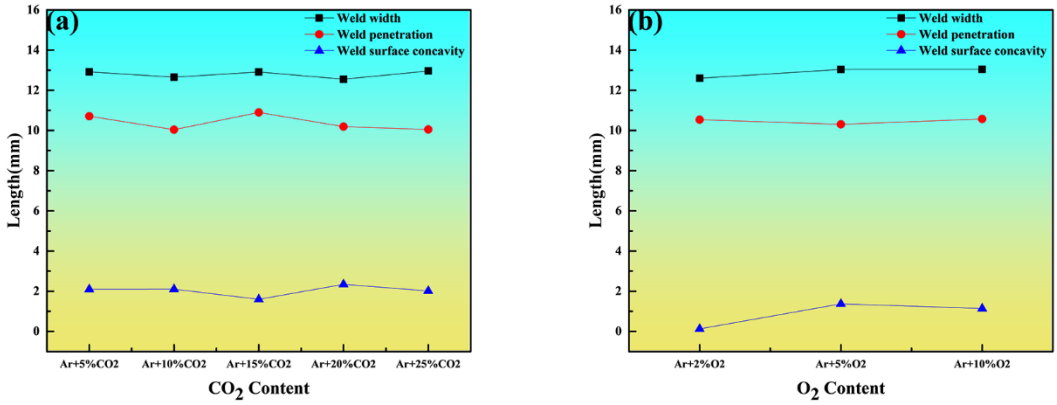

Fig. 14 Variations of weld bead width, penetration and surface concavity with different (a) CO_2 content and (b) O_2 content

The formation of the finger penetration and concave-shape weld bead surface is tightly related with the droplet transfer mode and arc pressure. The streaming spray transfer or spray transfer is the main transfer mode, in which the impact force is large enough to form a finger penetration, despite the relatively small droplet volume. According to Chen and Wu [20], the impact force of droplet is expressed as follow:

$$F_{imp} = \frac{f_d m_d V_d}{\pi {R_d}^2} \tag{6}$$

Where f_d is the droplet transfer frequency, m_d is the mass of the droplet, and V_d is

the velocity of droplet impinging on the welding pool.

The flow behavior of the welding pool under different droplet transfer mode is shown in Fig. 15. The droplet is smaller, and its transfer frequency is higher in streaming spray transfer mode. According to equation (6), the droplet impact force acting on the welding pool is very large, which results in a downward vortex and sunken welding pool surface given in Fig. 15(a) and is easy to produce a finger penetration and concave-shape weld bead surface. As shown in Fig. 15(b), due to the larger droplet and lower droplet transfer frequency, the droplet impacting force in this transfer mode is much less than that in streaming spray transfer mode. However, the arc length in projected spray transfer mode is smaller. Fan et al reported that the arc pressure decreased with increasing arc length [21], which means larger arc pressure in Fig. 15(b), and thus the similar weld formation could form.

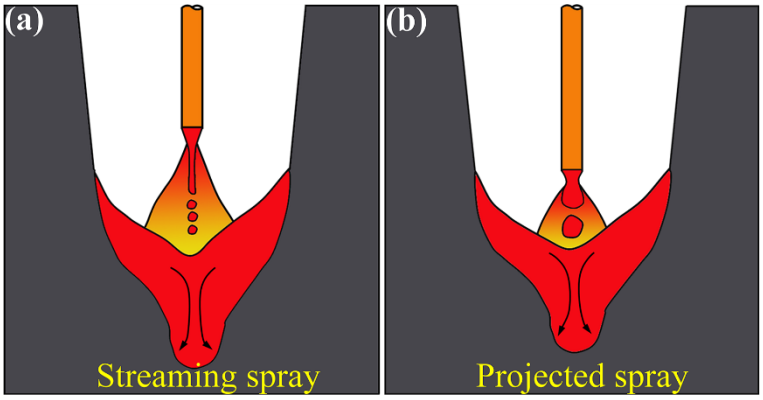

Fig.15 The flow behavior of the welding pool under (a) streaming spray droplet transfer and (b) projected spray droplet transfer.

4. Conclusions

(1) When the CO_2 or O_2 content in the shielding gas is low, the welding arc is

restrained by the narrow gap groove sidewalls, and climbs up along the sidewalls. With increasing CO_2 or O_2 content, the arc behavior takes on dramatic changes. The high CO_2 content leads to a more constricted arc.

(2) With the CO_2 content in the shielding gas increasing from 5% to 25%, the droplet transfer mode changes from projected spray to streaming spray. The droplet transfer mode keeps streaming spray transfer when the O_2 content ranges from 2% to 10%. The streaming spray transfer is accompanied by the long neck and arc jumping phenomenon.

(3) With increasing CO_2 or O_2 content, the weld bead surfaces changes slightly, but excessive O_2 content being added to the shielding gas results in a mass of slags on the weld surface, which may cause the inclusion defects or the lack-of-fusion defects in a multi-pass welded joint.

Abbreviations

NG-GMAW: Narrow-gap gas metal arc welding

GMAW: gas metal arc welding

DAS: data acquisition system

DCEP: direct-current electrode positive

W: weld width

H: weld penetration

C: weld surface concavity

F_g: gravity

r_d: the pendant droplet radius

ρ_d: the mass density of the droplet

g: the gravitational acceleration

F_γ: the surface tension

R_e: the radius of the electrode

γ: the surface tension coefficient of the liquid metal

F_d: the plasma drag force

C_d: the drag coefficient

ρ_g: the plasma gas density

v_g: the gas velocity

F_{emv}: the vertical component of electromagnetic force

μ_0 is the permeability in free space

I: the welding current

r_w: the radius of the wire

l_d: the length of the radius

F_{emr}: the radial component of electromagnetic force

RMS: root-mean-square

F_{imp}: the impact force of droplet

f_d: the droplet transfer frequency

m_d: is the mass of the droplet

V_d: the velocity of droplet impinging on the welding pool

Availability of data and materials

The datasets supporting the conclusions of this article are included within the article.

Competing interests

The authors declare no competing financial interests.

Funding

No applicable.

Authors' contributions

Xinhua Tang developed the idea, analyzed data, co-wrote and revised the paper. Guoqiang Liu developed the idea, designed and performed the experiments, analyzed data and wrote the paper. Qi Xu performed the experiments. Haichao Cui assisted with the experiments. Fenggui Lu assisted with paper revision.

Acknowledgements

Not applicable.

References

[1] Cui HC, Jiang ZD, Tang XH, Lu FG, Research on narrow-gap GMAW with swing arc system in horizontal position. International Journal of Advanced Manufacturing Technology 2014;74: 297-305.

[2] Guo N, Wang M, Guo W, Yu J, Feng J, Study on forming mechanism of appearance defects in rotating arc narrow gap horizontal GMAW. International Journal of Advanced Manufacturing Technology 2014;75(1-4): 15-20.

[3] Wang J, Sun Q, Zhang T, Zhang S, Liu Y, Feng J, Arc characteristics in alternating magnetic field assisted narrow gap pulsed GTAW. Journal of Materials Processing Technology 2018; 54: 54-264.

[4] Sathiya P, Mishra MK, Shanmugarajan B, Effect of shielding gases on microstructure and mechanical properties of super austenitic stainless steel by hybrid welding. Materials and Design 2012; 33:203-212.

[5] Huang HY, Effects of shielding gas composition and activating flux on GTAW weldments. Materials and Design 2009; 30:2404-2409.

[6] Zong R, Chen J, Wu C, Padhy GK, Influence of shielding gas on undercutting formation in gas metal arc welding. Journal of Materials Processing Technology 2016; 234: 169-176.

[7] Jonsson P, Murphy AB, Szekely J, The influence of O2 additions on argon-shielded gas metal arc welding processes. Welding Journal-Including Welding Research Supplement 1995;74 (2):48s.

[8] Wang LL, Lu FG, Wang HP, Murphy AB, Tang XH, Effects of shielding gas composition on arc profile and molten pool dynamics in gas metal arc welding of steels. Journal of Physics D: Applied Physics 2014;47(46): 465202

[9] Tusek J, Suban M, Experimental research of the effect of hydrogen in argon as a shielding gas in arc welding of high-alloy stainless steel. International journal of hydrogen energy 2000; 5(4): 369-376.

[10] Cai XY, Fan CL, Lin SF, Yang CL, Hu L, Ji XR, Effects of shielding gas composition on arc behaviors and weld formation in narrow gap tandem GMAW. International Journal of Advanced Manufacturing Technology 2017;91:3449-3456.

[11] Pires I, Quintino L, Miranda RM, Analysis of the influence of shielding gas mixtures on the gas metal arc welding metal transfer modes and fume formation

rate. Materials and Design 2007; 28:1623-1631.

[12] Wong YR, Ling SF, An investigation of dynamical metal transfer in GMAW—Effects of argon shielding gas. Journal of Materials Processing Technology 2014; 214:106-111.

[13] Murphy AB, Arundelli CJ. Transport coefficients of argon, nitrogen, oxygen, argon-nitrogen, and argon-oxygen plasmas. Plasma Chemistry and Plasma Processing 1994; 14(4): 451-490.

[14] Nemchinsky VA. Size and shape of the liquid droplet at the molten tip of an arc electrode. Journal of Physics D: Applied Physics 1994; 27(7): 1433.

[15] Scotti A, Ponomarev V, Lucas W. A scientific application oriented classification for metal transfer modes in GMA welding. Journal of Materials Processing Technology 2012; 212(6): 1406-1413.

[16] Y.S. Kim, T.W. Eagar, Analysis of metal transfer in gas metal arc welding. Welding Journal- New York 1993; 72 (6):269s–278s.

[17] Sahoo P, Debroy T, McNallan MJ, Surface tension of binary metal-surface active solute systems under conditions relevant to welding metallurgy. Metallurgical transactions B 1988; 19(3) 483-491.

[18] Rhee S, Kannatey-Asibu E. Observation of metal transfer during gas metal arc welding. Welding Journal- New York 1992; 71: 381-s.

[19] Amson J C. Lorentz force in the molten tip of an arc electrode. British Journal of Applied Physics 1965; 16(8): 1169.

[20] Chen J, Wu CS. Numerical analysis of forming mechanism of hump bead in high

speed GMAW. Welding in the World 2010; 54(9-10): R286-R291.

[21] Fan HG, Shi YW. Numerical simulation of the arc pressure in gas tungsten arc welding. Journal of Materials Processing Technology 1996; 61(3): 302-308.

Artwork and Tables with Captions

Fig. 1 (a) The schematic diagram of welding experiment system setup; (b) cross section dimension of specimen and its narrow-gap groove; (c) welding current and arc voltage waveforms; (d) characterization for first-pass weld bead of NG-GMAW.

Fig. 2 Variations of arc profile under shielding of gas mixtures with varied CO_2 contents

Fig. 3Variations of arc profile under shielding of gas mixtures with varied O_2 contents

Fig. 4Variations of arc length, arc width and arc area under shielding of gas mixtures with (a) varied CO_2 contents, and (b) varied O_2 contents

Fig.5Metal transfer process under shielding of gas mixtures of (a) Ar+5% CO_2 (b) Ar+10% CO_2

Fig.6 Schematic illustration of arc jumping phenomenon: (a) arc surrounding the bottom of droplet (b) force analysis when arc climbs to the top of neck. (c) droplet transfer after arc jumping.

Fig. 7Metal transfer process under shielding of gas mixtures of (a) Ar+15% CO_2; (b) Ar+20% CO_2;(c) Ar+5% CO_2

Fig. 8Schematic illustration of arc behavior and forces for (a) streaming spray transfer mode with low CO_2 content and (b) projected spray transfer mode with high CO_2 content

Fig. 9Metal transfer process under shielding of gas mixtures of (a) Ar+2% O_2; (b) Ar+5% O_2; (c) Ar+10% O_2

Fig. 10Current and voltage waveforms under shielding of (a) Ar+5% CO_2; (b) Ar+10% CO_2;(c) Ar+15% CO_2; (d) Ar+20% CO_2; (e) Ar+5% CO_2

Fig. 11Current and voltage waveforms under shielding of (a) Ar+2% O_2; (b) Ar+5% O_2; (c) Ar+10% O_2